IEEE Access
Multidisciplinary | Rapid Review | Open Access Journal

Received 27 March 2024, accepted 18 April 2024, date of publication 22 April 2024, date of current version 30 April 2024.

Digital Object Identifier 10.1109/ACCESS.2024.3392258

RESEARCH ARTICLE

Optimizing Motion Parameters in Soft Robotic Hands Using Bayesian Optimization: Enhancing Cycle Time, Addressing Vibration, and Repeatability

TOSHIHIRO NISHIMURA[1], (Member, IEEE), TATSUKI ISOGAI[2], YOSUKE SUZUKI[1], (Member, IEEE), TOKUO TSUJI[1], (Member, IEEE), AND TETSUYOU WATANABE[1], (Member, IEEE)

[1]Faculty of Frontier Engineering, Institute of Science and Engineering, Kanazawa University, Kakuma-Machi, Kanazawa 9201192, Japan
[2]Graduated School of Natural Science and Technology, Kanazawa University, Kakuma-Machi, Kanazawa 9201192, Japan

Corresponding authors: Toshihiro Nishimura (tnishimura@se.kanazawa-u.ac.jp) and Tetsuyou Watanabe (twata@se.kanazawa-u.ac.jp)

This work was supported by JSPS KAKENHI under Grant JP22K14220.

ABSTRACT This study proposes a novel motion optimization method for a manipulator equipped with a soft robotic hand for object transportation. The flexibility of the soft robotic hand induces large vibrations. The manipulator must pause until the vibration converges, leading to an increase in the cycle time. The robotic system also has issue with the low motion repeatability in the robotic hand, even under identical operational conditions. In this study, a method based on Bayesian algorithms is developed to optimize the motion of a manipulator. The objective is to minimize the cycle time for object transportation tasks, while considering the challenges of vibration and low repeatability in soft robotic hand systems. The optimization is performed through an exploratory search using actual experiments. To achieve a low-cost and versatile measurement system, this study proposes a method for deriving the cycle time, which is a key metric for optimization, based on the measurement results obtained using a web camera with standard specifications. The proposed optimization method is evaluated through a comparison with existing optimization methods, including the grid-search-based, conventional Bayesian optimization, particle swarm optimization, S. Lin's heuristic algorithm, and sparrow search algorithm. The proposed method achieves optimization results comparable in accuracy to those obtained using the grid-search-based optimization method, whereas requires 95% fewer searches. Furthermore, it provides more stable optimization results than those obtained using the conventional Bayesian optimization method.

INDEX TERMS Bayesian optimization, motion optimization, parameter tuning, soft robotic hand, vibration suppression.

I. INTRODUCTION

This study proposes a novel motion optimization method for a manipulator equipped with a soft robotic hand (soft robotic hand system), considering the issue of residual vibration in the soft robotic hand. The proposed method also addresses the low repeatability of the motion behaviors of soft robotic hand systems. In recent years, soft robotic hands constructed from materials such as silicone rubber have gained popularity owing to their high deformability, which makes them particularly effective for grasping fragile or complex-shaped objects [1], [2], [3], [4]. However, soft robotic hand systems face an issue that their high deformability often results in considerable vibrations during the motion of a robotic manipulator equipped with this type of hand. Vibration is induced during the acceleration and deceleration phases of

The associate editor coordinating the review of this manuscript and approving it for publication was Mohammad AlShabi.

TABLE 1. Comparison of the methods for suppressing residual vibration of robotic systems.

Approach		*Method*	*Special structures*	*Estimation of vibration properties in mechanical modeling (e.g., natural frequency)*	*Remark*
Software-based method	Using no mechanical model	**Proposed method**	✓Not required	✓Not required	See Table II
		PSO-based method* [22]		✓Not required	
		SHA-based method* [23]		✓Not required	
		BO-based method* [24]		✓Not required	
	Using mechanical model	Mechanical model-based [11][12][17]		✗Required (assumed to be given)	-
		Using high speed camera [14]-[16]		✗Required (obtained by sensors)	
		Using internal sensors [13][18]			
		SSA-based method* [19]		✗Required (identified by searching)	
		PSO-based method* [20]			
		BO-based method* [21]			
Hardware-based method		Installing additional structures or mechanisms [7]-[10]	✗Required	-	

* PSO, SHA, BO, and SSA refer to particle swarm optimization, S. Lin's heuristic algorithm, Bayesian optimization, and sparrow search algorithm, respectively.

the robotic manipulator movement. Residual vibrations in the soft robotic hand decrease the positioning accuracy. This reduced accuracy can lead to grasping failures, misalignments, and incorrect poses of the object during the release phase. Consequently, the manipulator needs to pause until residual vibrations subside during critical phases, such as grasping and releasing. The waiting time required for the residual vibrations to subside increases the cycle time, which is the time required to complete a series of robotic system actions. This study focuses on a transportation task performed using a soft robotic hand system. The goal is to develop a method that minimizes the cycle time of the system while accounting for hand vibrations. Another challenge in minimizing the cycle time in a soft robotic hand system is the low reproducibility of the motion. When the same motion commands are applied to a manipulator equipped with a soft robotic hand, the manipulator exhibits identical motion behavior. However, soft robotic hands produce different motion behaviors, resulting in varying cycle times. This is due to the flexibility of the soft robotic hand, where even slight positional deviations in the robotic manipulator can significantly impact the behavior of the hand. Several studies have proposed analytical models to estimate the motion behavior of soft robotic hands [5], [6]. However, an accurate estimation of the vibrational behavior of these hands using an analytical approach remains difficult because of the uncertainty caused by the low motion reproducibility. Therefore, to minimize the cycle time while accounting for the two challenges of vibration and low reproducibility, this study presents a novel method for optimizing the motion parameters of the robotic manipulator by utilizing data collected from real-world tests. The features of the proposed method are as follows.

- The manipulator motion is optimized by exploring the motion parameters to suppress residual vibration without relying on mechanical modeling.
- Optimization is achieved with minimal search trials, even when the criteria values are uncertain due to the low repeatability of soft robotic hands.

Tables 1 and 2 compare the proposed and existing methods in terms of vibration suppression techniques and motion optimization algorithms, respectively. As shown in Table 1, methods for suppressing the residual vibrations of robotic systems can be classified into hardware-based [7], [8], [9], [10] and software-based methods [11], [12], [13], [14], [15], [16], [17], [18], [19], [20], [21], [22], [23], [24]. The former methods target the soft robotic hand. They require special mechanisms or structures for vibration suppression, resulting in an increase in size and weight of the robotic hand. Hence, these methods cannot be applied if additional mechanisms or structures cannot be added. This study employs a software-based method. Software-based methods are classified into two types: those that involve mechanical modeling and those that do not. Several studies achieved vibration suppression using mechanical modeling given specific vibration properties [11] [12], [17]. The others [13], [18], [19], [20], [21], [22], [23], [24] proposed methods for identifying the vibration properties in mechanical models either through the use of sensors or by experimental exploration using an optimization algorithm. However, as described earlier, an accurate estimation of the vibrational behavior of soft robotic hands is challenging because of the low reproducibility of motion, which limits their adoption in soft robotic hand systems. Hence, a method that does not rely on mechanical modeling is effective for soft robotic hand systems. In [14], [15], and [16], the robotic manipulator motion was optimized to suppress the vibration of the target system using data collected from actual trials. Considering the need to minimize the number of actual trials, [14], [15], [16] have respectively employed the particle swarm optimization, S Lin's heuristic algorithm, and Bayesian optimization methods to efficiently search for optimal motion. This study develops a parameter-tuning method

TABLE 2. Comparison of exploratory motion optimization methods.

Method	*Number of trials for optimization*	*Addressing low-reproducibility problem*	*Remark*
Proposed method	✓Small	✓Yes	Compared in Section VI
Particle swarm Optimization [14]	✓Small	✗No	
S. Lin's heuristic algorithm [15]	✓Small	✗No	
Bayesian optimization method [16][25]-[28]	✓Small	✗No	
Sparrow search algorithm [38][39]	✓Small	✗No	
Grid-search-based optimization [30]	✗Large	✓Yes (if searching repeatedly)	
Extended Bayesian optimization method [29]	✓Small	✗No	*
Extended Bayesian optimization method [31][32]	✓Small	✗No	

* These methods cannot be adopted in the target system in this study because of the lack of the input parameter required for the search.

based on the Bayesian optimization algorithm [25], [26], [27], [28], [29], which is noted for its efficiency in parameter search among various optimization methods. As shown in Table 2, various other optimization methods can achieve optimization with a small number of search trials, although the issue of low-motion reproducibility has not been addressed, except by the grid search algorithm [30]. The grid search algorithm conducts a comprehensive search; hence, it can optimize the motion of systems with low motion reproducibility by repeatedly evaluating each parameter condition. An extended Bayesian optimization methods have also been developed [29], [30], [31], [32] to be applicable even when the criteria values do not correspond one-to-one to the search parameters. However, these methods do not address the special condition of unobservable noise (uncertainty) in the criterion values, which is the focus of this study. Therefore, no attempt has been made to develop an optimization method capable of tuning the parameters for soft robotic hand systems considering the uncertainties caused by low motion reproducibility and using a small number of search trials.

The primary contribution of this study is the development of a parameter optimization methodology for a soft robotic hand system with the aim of minimizing the operation cycle time while considering the vibrations and low motion reproducibility. This method refines the search for the optimal parameters by repeatedly revisiting previously evaluated conditions, thereby enhancing the reliability of the results and reducing the overall amount of exploration required. In addition, this paper proposes a novel, easily installable, and cost-effective system for measuring the vibrations of a robotic hand, which is a criterion for the optimization. References [18], [19], [20], [21], and [22] used expensive high-speed cameras and internal sensors requiring additional structures; conversely, this study uses a general-specification camera (30 fps, 640 × 360 pixels), thereby reducing costs.

II. PROBLEM DEFINITION

Fig. 1 shows the fundamental robotic system used in this study, including a 6-axis articulated robotic manipulator

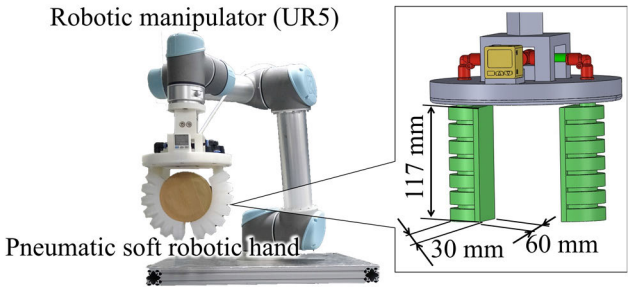

FIGURE 1. Target soft robotic hand system.

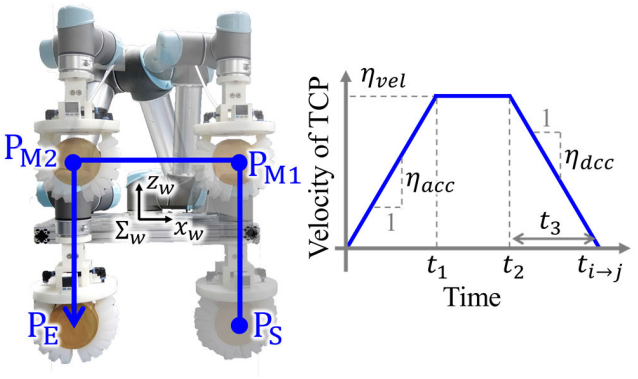

(a) Target trajectory

(b) Target velocity profile following the trapezoidal law

FIGURE 2. Target motion of the object transportation task.

(UR5) equipped with a pneumatic soft robotic hand. The target task is to transport an object grasped by a robotic hand using a robotic manipulator (Fig. 2). The soft robotic hand incorporates two bellows-structured fingers driven by pneumatic actuation inspired by [33] and [34], which is a widely used structure for pneumatic soft robotic hands. The fingers are made of a flexible and deformable material (Smooth-On, Dragon Skin 30), which is the same as that used in conventional pneumatic soft robotic hands. The target object is a cylinder (diameter: 102 mm, height: 50 mm, weight: 0.17 kg). Assuming object transportation within the pick-and-place task, the trajectory of the tool center point (TCP)

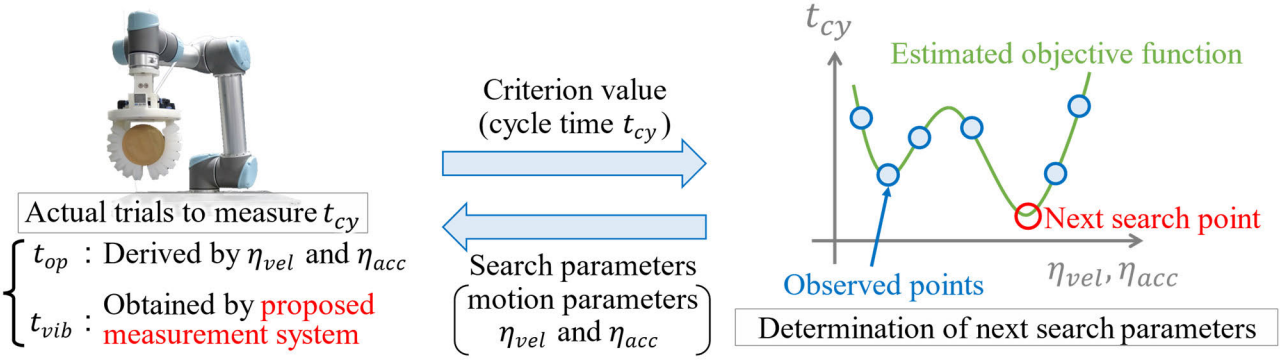

FIGURE 3. Illustration of the proposed method.

of the manipulator is set as a U-shaped path, as shown in Fig. 2(a). The operations for grasping and releasing objects are not considered in this study. P_S and P_E are the start and end points of the target trajectory, respectively; and P_{M1} and P_{M2} are the points at the corners of the U-shaped trajectory path. Let $\boldsymbol{p}_i (i = \{S, E, M1, M2\})$ be the coordinate of P_i relative to the world coordinate, Σ_w, shown in Fig. 2(a). The starting point $\boldsymbol{p}_s$ is set as follows:

$$\boldsymbol{p}_s = [p_{sx}, p_{sy}, p_{sz}]^{\mathrm{T}} \tag{1}$$

To form the U-shaped TCP path, the other points are expressed as follows:

$$\begin{aligned} \boldsymbol{p}_{\mathrm{M1}} &= \boldsymbol{p}_{\mathrm{s}} + [0, 0, d_1]^{\mathrm{T}} \\ \boldsymbol{p}_{\mathrm{M2}} &= \boldsymbol{p}_{\mathrm{M1}} - [d_2, 0, 0]^{\mathrm{T}} \\ \boldsymbol{p}_{\mathrm{E}} &= \boldsymbol{p}_{\mathrm{M2}} - [0, 0, d_1]^{\mathrm{T}} \end{aligned} \tag{2}$$

The TCP passes each point in the order of P_s, P_1, P_2, and P_E. The manipulator is controlled in such a way that the trajectories between each point are linear, and the velocity profile of the TCP within each linear path follows the trapezoidal law [35] (Fig. 2(b)). Let $\boldsymbol{p}_{\mathrm{TCP}}\left(t_{i\to j}\right)$ be the position of the TCP at time $t_{i\to j}$ after departing from P_i within the trajectory from P_i to P_j. The velocity $\dot{\boldsymbol{p}}_{\mathrm{TCP}}\left(t_{i\to j}\right)$ of the TCP is expressed as

$$\dot{\boldsymbol{p}}_{TCP}\left(t_{i\to j}\right) = \begin{cases} \eta_{acc}^{i\to j} t_{i\to j} \boldsymbol{e}_{i\to j} & if\ t_{i\to j} < t_1 \\ \eta_{vel}^{i\to j} \boldsymbol{e}_{i\to j} & else\ if\ t_{i\to j} < t_2 \\ \eta_{vel}^{i\to j} + \eta_{dcc}^{i\to j} t_3 & otherwise \end{cases} \tag{3}$$

where

$$\begin{aligned} \boldsymbol{e}_{i\to j} &= \frac{\boldsymbol{p}_j - \boldsymbol{p}_i}{\left\|\boldsymbol{p}_j - \boldsymbol{p}_i\right\|} \\ t_1 &= \eta_{vel}^{i\to j} / \eta_{acc}^{i\to j} \\ t_2 &= \frac{\left\|\boldsymbol{p}_j - \boldsymbol{p}_i\right\|}{\eta_{vel}^{i\to j}} - \frac{\eta_{vel}^{i\to j}}{2}\left(\frac{1}{\eta_{acc}^{i\to j}} + \frac{1}{\left|\eta_{dcc}^{i\to j}\right|}\right) \\ t_3 &= t_{i\to j} - t_2 \end{aligned} \tag{4}$$

$\eta_{vel}^{i\to j} (> 0)$, $\eta_{acc}^{i\to j} (> 0)$, and $\eta_{dcc}^{i\to j} (< 0)$ denote the maximum velocity, acceleration, and deceleration of the TCP movement following the trapezoidal law within the trajectory from P_i to P_j, respectively. In this context, the motion of the manipulator is determined by $\eta_{vel}^{i\to j}$, $\eta_{acc}^{i\to j}$, and $\eta_{dcc}^{i\to j}$ for the three linear paths within the U-shaped trajectory, i.e., nine motion parameters. Correspondingly, the time t_{op}, required for the manipulator to accomplish the U-shaped trajectory movement is given by

$$t_{op} = \sum\nolimits_{i,j} \left(t_2 + \frac{\eta_{vel}^{i\to j}}{\left|\eta_{dcc}^{i\to j}\right|}\right) \tag{5}$$

For a manipulator with a rigid robotic hand, the cycle time is equivalent to t_{op} because the vibration of the robotic hand after reaching the endpoint is negligibly small, allowing the subsequent release motion to be performed immediately. In contrast, with a soft robotic hand, the manipulator must pause until the vibration in the hand converges to a low level, thereby increasing the overall cycle time. This causes an increase in the actual cycle time. Let t_{vib} be the time required for the vibration to converge. Then, the actual cycle time, t_{cy}, is expressed as

$$t_{cy} = t_{op} + t_{vib} \tag{6}$$

Although t_{op} can be reduced by adjusting the motion parameters for the high-speed operation of the manipulator, the high-speed motion can cause significant vibration in the robotic hand, thereby increasing t_{vib} and leading to an increased t_{cy}. In contrast, reducing the speed of the movements of the manipulator can suppress the vibrations, but this will result in a longer t_{op} and, consequently, an increased t_{cy}.

Considering this tradeoff relationship, this study challenges to optimize the motion parameters for minimize t_{cy}. In this study, for the simplicity, the maximum velocities, accelerations, and decelerations for each linear path are set to be same value each other, and the magnitude of the acceleration is set to be equal to that of deceleration:

$$\begin{aligned} \eta_{vel}^{\mathrm{S}\to\mathrm{M1}} &= \eta_{vel}^{\mathrm{M1}\to\mathrm{M2}} = \eta_{vel}^{\mathrm{M2}\to\mathrm{E}} := \eta_{vel} \\ \eta_{acc}^{\mathrm{S}\to\mathrm{M1}} &= \eta_{acc}^{\mathrm{M1}\to\mathrm{M2}} = \eta_{acc}^{\mathrm{M2}\to\mathrm{E}} := \eta_{acc} \\ \eta_{dcc}^{\mathrm{S}\to\mathrm{M1}} &= \eta_{dcc}^{\mathrm{M1}\to\mathrm{M2}} = \eta_{dcc}^{\mathrm{M2}\to\mathrm{E}} := \eta_{dcc} \\ \eta_{acc} &= -\eta_{dcc} \end{aligned} \tag{7}$$

III. OVERVIEW OF PROPOSED METHODOLOGY

Fig. 3 illustrates the overview of the proposed method, which optimizes the motion parameters (η_{vel} and η_{acc}) to minimize the cycle time (t_{cy}) in the object transportation task. This method addresses the challenges of vibration and low motion repeatability in soft robotic hand systems by exploring the optimal parameters via experimental trials. This method is based on Bayesian optimization, which is adopted to reduce the number of trials. Let $\boldsymbol{s}$ be the search parameter:

$$\boldsymbol{s} = [\eta_{vel}, \eta_{acc}] \tag{8}$$

confined within domain S:

$$S = \left\{\boldsymbol{s}^1, \boldsymbol{s}^2, \boldsymbol{s}^3, \ldots, \boldsymbol{s}^l\right\} \tag{9}$$

The objective function is denoted as $t_{cy}(\boldsymbol{s})$. Bayesian optimization determines the optimal parameter $\boldsymbol{s}_{opt}$ yielding the optimal $t_{cy}(\boldsymbol{s}_{opt})$ through a sequential search with a small number of trials. Let $\boldsymbol{s}^i_{act}$ ($\in S_{act} = \{\boldsymbol{s}^1_{act}, \boldsymbol{s}^2_{act}, \ldots\}$) represent the investigated search parameters with known corresponding $t_{cy}(\boldsymbol{s}^i_{act})$. Then, $t_{cy}(\boldsymbol{s})$ for all search parameters in S is estimated using a Gaussian process. Using the estimated $t_{cy}(\boldsymbol{s})$, the method determines the next search parameter to be explored. By considering the profile of the estimated $t_{cy}(\boldsymbol{s})$ and the distribution of $\boldsymbol{s}^i_{act}$ in the search domain to determine the next search parameter, the method achieves the optimization with fewer trials. This approach is applicable even when the objective function is a black-box function.

In the soft robotic hand system, the cycle time (t_{cy}) obtained from experiments may lack reliability due to the low repeatability in the soft robotic hand. To address this issue, the proposed method re-evaluates the previously investigated search parameters selectively based on the estimated objective function $t_{cy}(\boldsymbol{s})$, rather than randomly. This re-evaluation strategy for soft robotic hand systems leads to more reliable optimization results with fewer trials.

t_{op} in (6) can be derived from (5) using the search parameters, η_{vel} and η_{acc}. For efficiency, the vibration time (t_{vib}) is measured experimentally, whereas t_{op} is calculated computationally in each trial to determine the total cycle time (t_{cy}). This study aims to develop an easily installable and cost-effective measurement system for vibration time (t_{vib}) using a standard (general specification) camera as an external sensor. The subsequent sections describe the proposed system for measuring the cycle time and methodology for optimizing the motion parameters.

IV. CYCLE TIME MEASUREMENT METHOD

This section describes the derivation of the cycle time (t_{cy}), which is calculated from the robot operation time (t_{op}) and vibration time (t_{vib}). As t_{op} can be computationally calculated, this section focuses on the experimental measurement of t_{vib}. Fig. 4 illustrates the measurement system used for t_{vib}. A camera (Logicool, BRIO) is positioned to capture images of the robotic hand when the TCP reaches the endpoint (P_E) of the motion trajectory. In tasks such as object transportation,

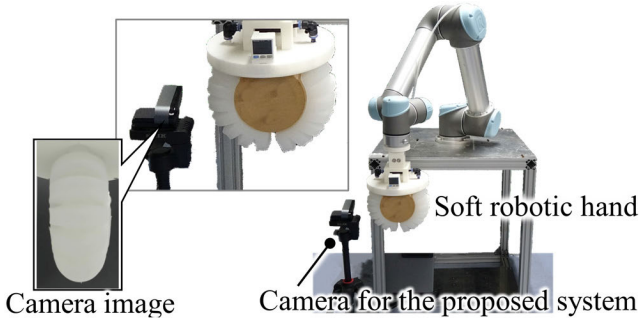

FIGURE 4. Proposed measurement system for determining the vibration convergence time.

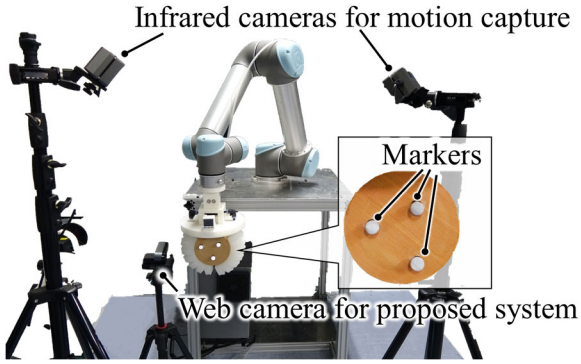

FIGURE 5. Experimental setup for evaluating the proposed measurement system.

a high positioning accuracy at the endpoint P_E is crucial. Therefore, the vibrational behavior of the robotic hand is observed when the TCP is at P_E. The camera setup can be adjusted for various tasks. The camera begins to capture images of the robotic hand as the TCP reaches P_E. The image captured by the camera at time step t is represented by $\boldsymbol{M}_t$, which belongs to $\mathbb{R}^{W\times H}$ and has a resolution of $W \times H$ [pix]. To evaluate the vibration magnitude, the difference E_t between the images at two consecutive time steps is calculated at each time step, as follows:

$$E_t = \sqrt{\sum_W \sum_H \left(\boldsymbol{M}_{t(w,h)} - \boldsymbol{M}_{t-1(w,h)}\right)^2} \tag{10}$$

If the displacement of the robotic hand between the tth and $(t-1)$th time steps is large due to its large vibration, E_t becomes large, and vice versa. Thus, the extent of the vibration can be estimated by monitoring the E_t value. t_{vib} is identified at the point where the value of E_t decreases to a predefined threshold, E_{th}. t_{vib} is then defined as the moment at which E_t decreases below E_{th}:

$$E_t \mid_{t=t_{vib}} < E_{th} \tag{11}$$

A. VALIDATION

This section validates the proposed methodology for measuring the vibration time (t_{vib}). The reliability of the operation time (t_{op}) derivation is considered high, given the use of the industrial robotic manipulator UR5, which is a widely recognized standard in the industry. Fig. 5 shows the experimental

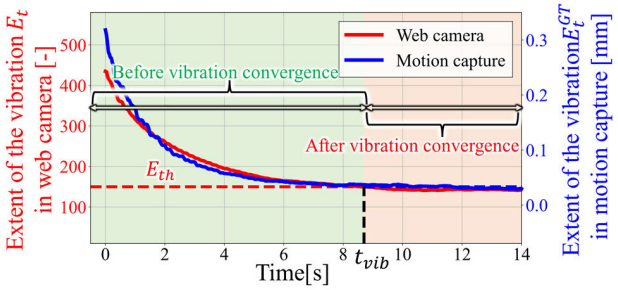

(a) Extent of vibration measured using the proposed and motion capture measurement systems E_t and E_t^{GT}

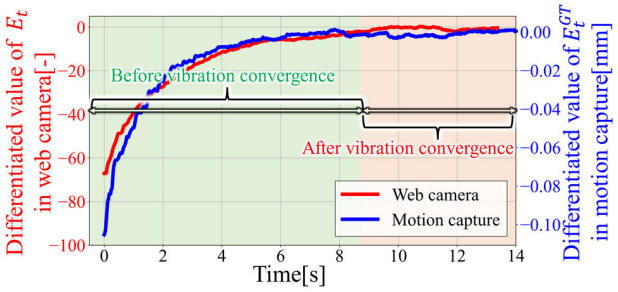

(b) Numerical differentiated values of E_t and E_t^{GT}

FIGURE 6. Comparison of vibration measurements in the soft robotic hand using the proposed and motion capture systems.

setup used to evaluate the t_{vib} measurement method. In the experiment, a motion capture system (OptiTrack PrimeX 13) was used alongside the proposed system to measure the vibration behavior. The motion-capture system tracks the positions of the reflective markers attached to the grasped object using infrared cameras. Let $\boldsymbol{p}_{mk} \in \mathbb{R}^3$ be the center of gravity of these markers relative to the world coordinate system, Σ_w, shown in Fig. 2. The manipulator executes the object transportation task with $\eta_{vel} = 700$ [mm/s] and $\eta_{acc} = 1700$ [mm/s^2]. Upon the TCP reaching the end point $\mathrm{P_E}$ of the movement trajectory, both the proposed and motion capture systems begin to measure the vibrational behavior of the robotic hand and grasped object. The converged position $\bar{\boldsymbol{p}}_{mk} \in \mathbb{R}^3$ represents the stable position of $\boldsymbol{p}_{mk}$ after a sufficient time has elapsed. The displacement $\Delta\boldsymbol{p}_{mk}$, indicating the movement of the robotic hand and object relative to the stable position, is then calculated as follows:

$$\Delta\boldsymbol{p}_{mk} = \boldsymbol{p}_{mk} - \bar{\boldsymbol{p}}_{mk} \tag{12}$$

Then, the effective value E_t^{GT} of the vibration during the small time Δt at the tth time step is given by:

$$E_t^{GT} = \sqrt{\frac{1}{\Delta t}\int_{\Delta t} \left\|\Delta\boldsymbol{p}_{mk}\right\|^2 dt} \tag{13}$$

The motion capture system had a sufficiently high sampling rate (1 kHz) to measure the vibration behavior of the robotic hand and object. Thus, E_t^{GT}, which represents the ground truth of the vibration behavior, is consistent with the actual vibration behavior. Therefore, the accuracy of E_t was assessed by comparing its behavior with that of E_t^{GT}. Fig. 6(a) shows the results for both E_t and E_t^{GT}, indicating that their values decreased over time and eventually stabilized at specific levels. Fig. 6(b) shows the numerically differentiated values of E_t and E_t^{GT} based on the data shown in Fig. 6(a). The declines in both E_t and E_t^{GT} ceased at approximately the same time, indicating that the proposed methodology effectively assessed the vibration magnitude. The threshold value E_{th}, used in (11) to determine the vibration time t_{vib}, was set to 150 to ensure that the vibration magnitude remained below 0.06 mm.

V. PARAMETER OPTIMIZATION METHOD

This section introduces the proposed method for optimizing the motion parameters, $\boldsymbol{s} = [\eta_{vel}, \eta_{acc}]$, to minimize the cycle time $t_{cy}(\boldsymbol{s})$. This optimization is achieved by iteratively evaluating $t_{cy}(\boldsymbol{s})$ through actual experiments using a Bayesian-optimization-based algorithm. The manipulator performs the transportation operation with a given parameter $\boldsymbol{s}$. Subsequently, $t_{cy}(\boldsymbol{s})$ is calculated by combining the operation time $t_{op}(\boldsymbol{s})$, as defined in (5), and the vibration time $t_{vib}(\boldsymbol{s})$, which is measured using the proposed system detailed in Section IV. Notably, $t_{vib}(\boldsymbol{s})$ encompasses the uncertainties caused by the low-repeatability characteristic of the soft robotic hand system. The expression for $t_{cy}(\boldsymbol{s})$ is as follows:

$$t_{cy}(\boldsymbol{s}) = \bar{t}_{cy}(\boldsymbol{s}) + \Delta e \tag{14}$$

where $\bar{t}_{cy}$ is the mean value of $t_{cy}(\boldsymbol{s})$, and Δe is the error following the unknown probabilistic distribution. The objective of this optimization is as follows:

$$\boldsymbol{s}_{opt} = \underset{s\in S}{\operatorname{argmin}}\, \bar{t}_{cy}(\boldsymbol{s}) \tag{15}$$

Next, the optimization procedure is described. Let $\boldsymbol{s}_n$ and $t_{cy}(\boldsymbol{s}_n)$ be $\boldsymbol{s}$ and $t_{cy}(\boldsymbol{s})$ in the nth search, respectively. Although the obtained $t_{cy}(\boldsymbol{s})$ includes the error Δe as shown in (14), it is used as the criterion value J_n for the Bayesian optimization algorithm:

$$J_n = t_{cy}(\boldsymbol{s}_n) \tag{16}$$

The mean $\mu_n(\boldsymbol{s})$ and variance $\sigma_n^2(\boldsymbol{s})$ of the estimated objective function (i.e., $t_{cy}(\boldsymbol{s}_n)$) are given by

$$\mu_n(\boldsymbol{s}) = \boldsymbol{k}_n(\boldsymbol{s})\left(\boldsymbol{K}_n + \boldsymbol{I}_n\sigma_\omega^2\right)^{-1}\boldsymbol{J}_n \tag{17}$$

$$\sigma_n^2(\boldsymbol{s}) = k(\boldsymbol{s},\boldsymbol{s}) - \boldsymbol{k}_n(\boldsymbol{s})\left(\boldsymbol{K}_n + \boldsymbol{I}_n\sigma_\omega^2\right)^{-1}\boldsymbol{k}_n^{\mathrm{T}}(\boldsymbol{s}) \tag{18}$$

where

$$\boldsymbol{J}_n = [J_1, J_2 \ldots, J_n]^{\mathrm{T}}$$

$$\boldsymbol{K}_n = \begin{bmatrix} k(\boldsymbol{s}_1,\boldsymbol{s}_1) & \cdots & k(\boldsymbol{s}_1,\boldsymbol{s}_n) \\ \vdots & \ddots & \vdots \\ k(\boldsymbol{s}_n,\boldsymbol{s}_1) & \cdots & k(\boldsymbol{s}_n,\boldsymbol{s}_n) \end{bmatrix}$$

$$\boldsymbol{k}_n = [k(\boldsymbol{s},\boldsymbol{s}_1), k(\boldsymbol{s},\boldsymbol{s}_2), \ldots, k(\boldsymbol{s},\boldsymbol{s}_n)]$$

$$k(\boldsymbol{s}_i,\boldsymbol{s}_j) = \exp\left(-\frac{\left\|\boldsymbol{s}_i - \boldsymbol{s}_j\right\|}{2\gamma^2}\right) \tag{19}$$

and $\boldsymbol{I}_n \in \mathbb{R}^{n\times n}$ denotes an identity matrix [7]. σ_ω and γ are the hyper parameters. Considering the uncertainties in t_{cy}, the mean value of the objective function $\bar{t}_{cy}(\boldsymbol{s})$ is expressed as

$$\bar{t}_{cy}(\boldsymbol{s}) \sim \mathcal{N}\left(\mu_n(\boldsymbol{s}), \sigma_n^2(\boldsymbol{s})\right) \tag{20}$$

To obtain the parameters that minimize the objective function, the lower confidence bound (LCB) function $l_n(\boldsymbol{s})$, is used as the acquisition function:

$$l_n(\boldsymbol{s}) = \mu_n(\boldsymbol{s}) - \theta(n)\,\sigma_n(\boldsymbol{s}) \tag{21}$$

The next search parameter $\boldsymbol{s}_{n+1}$ is determined by

$$\boldsymbol{s}_{n+1} = \underset{\boldsymbol{s}}{\operatorname{argmin}}\, l_n(\boldsymbol{s}) \tag{22}$$

$\theta(n)$ in (21) represents the weight that balances the emphasis between exploration and exploitation. Setting a larger $\theta(n)$ favors exploratory search, leading to the selection of parameters from the less densely searched areas of the domain. Conversely, setting a smaller $\theta(n)$ encourages exploitational search, prioritizing parameters that are more likely to minimize the objective function. Therefore, the determination of $\theta(n)$ is critical for identifying the optimal search parameter. The special function of $\theta(n)$ used in the proposed method is set as follows:

$$\theta(n) = \delta\beta\sqrt{\frac{\log n}{n}}$$
$$\delta = \begin{cases} 1 & if\ n < \tau_{th} \sim U(0,\tau) \\ 0 & otherwise \end{cases} \tag{23}$$

where β is a constant value (hyper parameter), and $U(0,\tau)$ represents a uniform distribution with the bounds ranging from 0 to τ. The coefficient $\beta\sqrt{\log n/n}$ is often used in the optimization method based on the Bayesian optimization [36]. This coefficient decreases with an increasing number of searches (n), facilitating a shift from exploratory to exploitative searches. This approach helps prevent the optimization from settling at a local minimum. However, it does not address the issue of the low reliability of the obtained criterion (objective function) values. To overcome this, an additional coefficient, δ, is introduced. In each search, δ is randomly set to either 0 or 1. If the number of trials (searches), n, is less than a threshold τ_{th}, following a uniform distribution $U(0,\tau)$, δ is set to 1; otherwise, it is set to 0. With $\delta = 1$, the policy for selecting the next search parameter aligns with the traditional LCB-based approach, which avoids revisiting previously searched parameters until the optimization nears the vicinity of the optimal parameter. Conversely, with $\delta = 0$, the acquisition function is equivalent to the estimated mean objective function:

$$l_n(\boldsymbol{s}) = \mu_n(\boldsymbol{s}) \tag{24}$$

In this methodology, the next search parameter is primarily determined based on the LCB function, $l_n(\boldsymbol{s},\delta = 1)$, which is consistent with the conventional Bayesian optimization. However, to address the uncertainties inherent in the objective function of the target system, the mean function $\mu_n(\boldsymbol{s})$ is intermittently used to select the next search parameter, increasing the likelihood of re-investigating previously searched parameters. The re-investigated search parameters provide different criterion values from those yielded by the previously searched parameters because of the low repeatability. $\mu_n(\boldsymbol{s})$ is updated to estimate the objective function, considering the different criteria obtained through the re-investigation. Thus, this approach enhances the reliability of the estimated objective function ($\mu_n(\boldsymbol{s})$), particularly when the obtained objective function values are uncertain. The search parameters are re-investigated more frequently as the number of trials n, increases, as shown in (23). Consequently, this method improves the reliability of the estimated objective function while effectively managing the number of trials. In contrast, in systems where the objective function values are certain, as in conventional studies, re-investigating the previously searched parameters is redundant because the criterion value remains unchanged.

Algorithm: Bayesian-algorithm-based optimization using re-investigation

Input: Initial search parameter $\boldsymbol{s}_1 = \{\eta_{vel1}, \eta_{acc1}\}$
Search domain S
Hyper parameters $\beta = 30$, $\tau = 100$, $\gamma = 0.7$, $\sigma_\omega^2 = 0.1$, $\tau_{th} = 80$, and $m_{th} = 10$

While
  Investigate the criterion value $J_n = t_{cy}(\boldsymbol{s}_n)$ using the actual experiment
  Add J_n to $\mathcal{J}(\boldsymbol{s}_n)$
  If $|\mathcal{J}(\boldsymbol{s}_n)| < m_{th}$
    Calculate μ_n, σ_n, and l_n
    Calculate l_n using $\delta = 0$ or 1
    Determine the next search parameter: $\boldsymbol{s}_{n+1} = \operatorname{argmin} l_n$
  Else if $|\mathcal{J}^{(\boldsymbol{s}_n)}| = m_{th}$
    break
Loop
Determine the optimal parameter: $\boldsymbol{s}_{opt} = \underset{\boldsymbol{s}\in S}{\operatorname{argmax}}|\mathcal{J}(\boldsymbol{s})|$ (corresponding to $\boldsymbol{s}_{opt} = \boldsymbol{s}_n$)
Calculate optimal criterion value $t_{cy}(\boldsymbol{s}_{opt}) = \frac{1}{|\mathcal{J}(\boldsymbol{s})|}\sum_{J\in\mathcal{J}(\boldsymbol{s})} J$

FIGURE 7. Proposed optimization method.

Finally, the condition for terminating the optimization process and the policy for determining the optimal parameters are described. Let $\mathcal{J}(\boldsymbol{s})$ represent the set of criterion values obtained for a specific search parameter $\boldsymbol{s}$. The size of this set, $|\mathcal{J}(\boldsymbol{s})|$, corresponds to the number of times that $\boldsymbol{s}$ is investigated using the algorithm. The optimization process terminates when the count $|\mathcal{J}(\boldsymbol{s})|$ reaches its threshold, m_{th}:

$$|\mathcal{J}(\boldsymbol{s})| = m_{th} \tag{25}$$

The rationale behind this termination condition is that the more frequently a parameter is investigated, the higher its likelihood of being optimal. The optimal parameter $\boldsymbol{s}_{opt}$ is given by

$$\boldsymbol{s}_{opt} = \underset{\boldsymbol{s}\in S}{\operatorname{argmin}}\,|\mathcal{J}(\boldsymbol{s})| \tag{26}$$

Note that $\max|\mathcal{J}(\boldsymbol{s})| = m_{th}$. The optimal cycle time is given by

$$t_{cy}(\boldsymbol{s}_{opt}) = \frac{1}{|\mathcal{J}(\boldsymbol{s})|}\sum\nolimits_{J\in\mathcal{J}(\boldsymbol{s})} J \tag{27}$$

The proposed methodology is summarized in Fig. 7.

VI. EVALUATION

This section presents the evaluation of the proposed method, which was designed to minimize the cycle time of the object transportation task performed by the soft robotic hand system. The effectiveness of this method was assessed by comparing it with existing optimization techniques. For this evaluation, the range of the search parameters, specifically the motion parameters of the manipulator, were defined as follows:

$$S = \left\{ \boldsymbol{s} = [\eta_{vel}, \eta_{acc}] \,|\, \begin{matrix} \eta_{vel} = \{100, 200, \cdots 900\} \\ \eta_{acc} = \{1500, 1700 \cdots 3700\} \end{matrix} \right\} \tag{28}$$

The maximum velocities (η_{vel}) of the TCP were set in the range from 100 mm/s to 900 mm/s, with increments of 100 mm/s. The accelerations (decelerations) (η_{acc}) were set in the range from 1500 to 3700 mm/s^2, with increments of 200 mm/s^2. This resulted in a total of 108 distinct parameter settings. The effectiveness of the proposed method for the optimization of soft robotic hand systems is evaluated through a comparison with the existing optimization methods listed in Table 2. Given the extensive number of experiments required for a comprehensive comparison, an evaluation was conducted using a simulator developed based on actual experimental data. In the following subsections, the construction of the evaluation simulator is described, and the comparative evaluation using the constructed simulator is presented.

A. CONSTRUCTION OF EVALUATION SIMULATOR

To conduct the evaluation efficiently, a simulator was constructed based on the relationship between the cycle times and search parameters derived from actual experimental data. The experimental setup is illustrated in Fig. 4 and described in Section II. The object transportation task was conducted for each parameter setting. The cycle times were measured using the proposed measurement system described in Section IV. For each setting of the search parameters, the experiments to measure the cycle time were conducted 10 times. Fig. 8 shows the results of the cycle-time profile, including the means and errors. As indicated by the data, varying cycle times were observed even for the same search parameters, demonstrating the low repeatability of the soft robotic hand system. To construct a simulator model that represents these results, the means ($\mu_{GT}(\boldsymbol{s})$) and variances ($\sigma^2_{GT}(\boldsymbol{s})$) of the obtained cycle times for each parameter set $\boldsymbol{s}$ were calculated. Assuming a normal distribution for the cycle times obtained for each $\boldsymbol{s}$, the simulated cycle time, t^{sim}_{cy}, is given by

$$t^{sim}_{cy}(\boldsymbol{s}) \sim \mathcal{N}\left(\mu_{GT}(\boldsymbol{s}), \sigma^2_{GT}(\boldsymbol{s})\right) \tag{29}$$

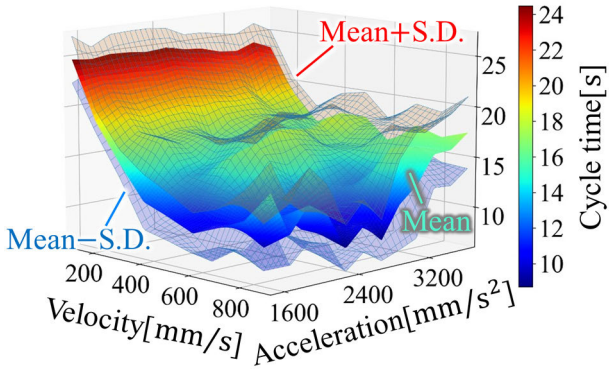

FIGURE 8. Result of mean and standard deviation (S.D.) of the cycle times obtained from the actual experiments.

Notably, while the constructed simulator is based on the assumption that the cycle time variation follows a normal distribution, the proposed optimization methodology, designed to address the issue of low repeatability, can also be applied to scenarios where the cycle time follows other distributions.

B. COMPARISON WITH EXISTING METHODS

This section evaluates the proposed methodology by comparing it with six existing optimization methods. These include two grid-search-based methods (GS1 and GS10 methods) and four conventional optimization methods: the Bayesian algorithm method (BA), particle swarm optimization (PSO), S. Lin's heuristic algorithm (SHA), and the sparrow search algorithm (SSA). Brief descriptions of the algorithms used in each method are provided as follows:

1) GRID-SEARCH-BASED METHODS (GS1 AND GS10 METHODS)

The GS1 and GS10 methods aim to identify the optimal parameter by examining the objective function values across all search parameter conditions. The GS1 method selects the optimal parameter with the minimum cycle time based on the data from a single experiment conducted for each search parameter. In contrast, the GS10 method determines the optimal parameter based on the minimum cycle time derived from aggregating data across 10 experiments for each parameter, which improves the reliability of the resulting optimal parameter.

2) CONVENTIONAL BAYESIAN-ALGORITHM-BASED METHOD (BA METHOD)

The BA method utilizes the Bayesian algorithm to optimize the search parameters. The exploration process in this method is similar to that of our proposed method and employs the following conventional LCB function as the acquisition function:

$$l_n(\boldsymbol{s}) = \mu_n(\boldsymbol{s}) - \beta\sqrt{\frac{\log n}{n}}\sigma_n(\boldsymbol{s}) \tag{30}$$

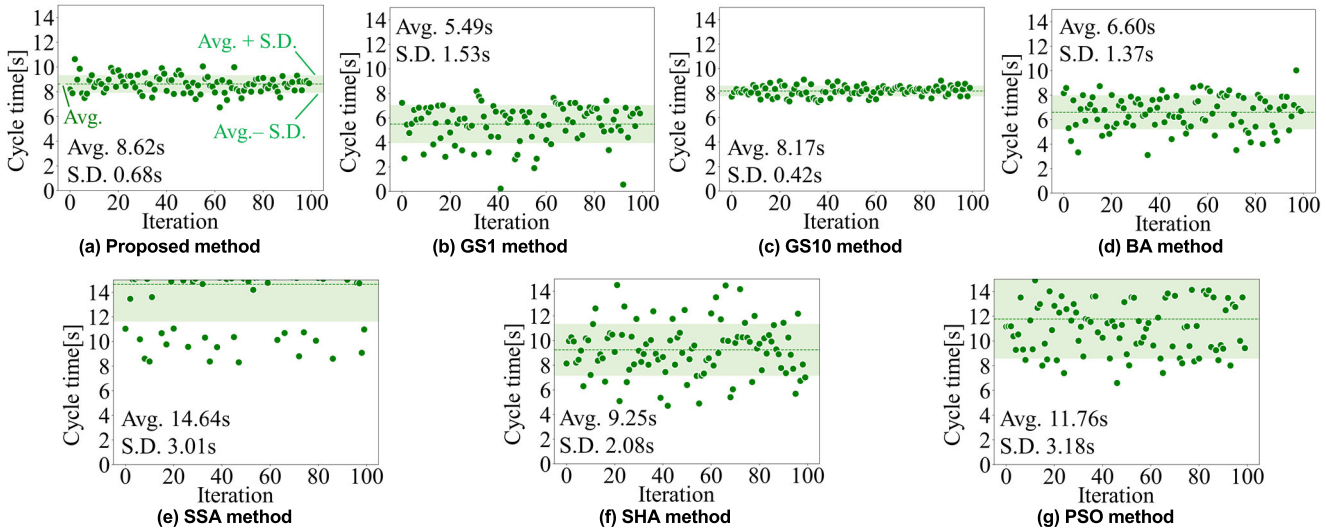

FIGURE 9. Result of the optimal value, i.e., minimum cycle time, with the optimal search parameters obtained using each method.

The optimization process is terminated when the previously investigated search parameter is selected as the next search parameter, i.e., the parameter search is repeated.

3) PARTICLE SWARM OPTIMIZATION METHOD (PSO METHOD)

The PSO method searches for optimal parameters by updating the particle positions corresponding to the candidate optimal parameters [37]. The position of each particle is updated based on its own best position and the best position in the all particles. In this study, the search was terminated when all the particles are within less than the threshold distance from their centroid.

4) S. LIN'S HEURISTIC-ALGORITHM-BASED METHOD (SHA METHOD)

The SHA method combines a random search and heuristic algorithms. In each step, several search conditions are evaluated, and then some of the variables in the search condition that provide the best criteria values in the previous evaluation are changed to random values. The optimal parameters are determined by repeating this procedure.

5) SPARROW SEARCH ALGORITHM-BASED METHOD (SSA METHOD)

The SSA method is a recently developed technique inspired by the behavior of sparrows [38], [39]. Similar to the PSO method, the position of the candidate optimal parameter (sparrow) is updated based on the criteria. The sparrows are divided into producers and scroungers. This method utilizes the differences in the behaviors of producers and scroungers for an efficient search.

To assess the effectiveness of each optimization method in a system with low repeatability, 100 simulated experiments based on (29) were conducted for each method to determine the optimal value. For the proposed and existing methods, except for the GS1 and GS 10 methods, the initial search parameters were randomly set for each experiment. The results are summarized in Figs. 9 and 10, and Table 3. Fig. 9 illustrates the optimal cycle times achieved by each method over the iterations. The variations in these values are also depicted in the figure, where the proposed and GS10 methods exhibit smaller variances than the other methods. Fig. 10 shows the distribution of optimal search parameters for each method, where the parameters of the proposed method are predominantly clustered around specific values, such as $[\eta_{vel}, \eta_{acc}] = [900, 2300]$ and $[900, 2700]$. For the quantitative comparison, three performance indicators, N_{inv}, R_{nearGS10}, and R_{clust}, are introduced (Table 3). N_{inv} represents the number of investigations required to identify the optimal search parameter in each experiment. A smaller N_{inv} indicates a faster search. R_{nearGS10} represents the proportion of experiments in which the optimized cycle time falls within the 3-sigma limit of the cycle time optimized using the GS10 method. Given that the cycle time optimized by the GS10 method serves as a benchmark, R_{nearGS10} measures the accuracy of each method in comparison to this benchmark.

Letting $\mu_{\mathrm{GS10}}(= 8.17\,\mathrm{s})$ and $\sigma_{\mathrm{GS10}}(= 0.42)$ be the mean and standard deviation of the optimal cycle times

TABLE 3. Performance indicators for each optimization method.

	N_{inv} (CV*)	R_{nearGS10}	R_{clust}
Proposed	35.3 (0.21)	88%	89 %
GS1	108 (0)	14 %	44 %
GS10	1080 (0)	-	92 %
BA	15.9 (0.21)	45 %	48 %
SSA	899.5 (1.88)	7 %	85 %
SHA	42 (0)	41 %	35 %
PSO	154.1 (3.35)	23 %	41 %

* Coefficient of variation

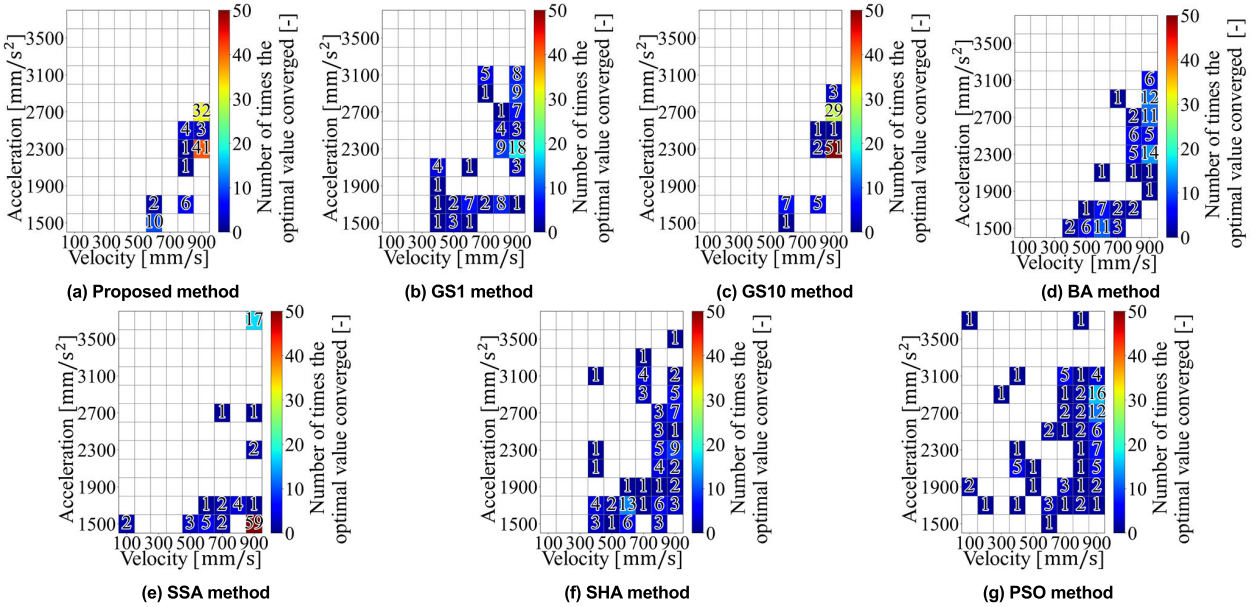

FIGURE 10. Result of the number of times the optimal value converged in the optimal search for each search parameter.

for GS10 method, respectively (see Fig. 9(c)), R_{nearGS10} is expressed by:

$$R_{\text{nearGS10}} = \frac{\sum_i \phi_i}{\text{Num. of experiments } (= 100)}$$
$$\phi_i = \begin{cases} 1 & \text{if } \rho_i < 3\sigma_{\text{GS10}} \\ 0 & \text{otherwise} \end{cases}$$
$$\rho_i = \left| t_{cy}\left(\boldsymbol{s}_{opt}\right)_i - \mu_{\text{GS10}} \right| \tag{31}$$

where $t_{cy}\left(\boldsymbol{s}_{opt}\right)_i$ is the optimal cycle time obtained in the ith experiment. R_{clust} represents the proportion of experiments that converged to the top four parameter conditions based on the frequency of convergence, relative to the total number of experiments conducted. R_{clust} indicates the degree of clustering (or variation) of the parameter conditions yielding the optimal cycle time for each method. As presented in Table 3, only the proposed method yielded high R_{nearGS10} and R_{clust} with a small N_{inv}. Notably, the GS10 method is the benchmark; thus, it yields high R_{nearGS10} and R_{clust} although it requires a large N_{inv}. The SSA method yielded high R_{clust} but low R_{nearGS10}. The parameter conditions that provided the optimal cycle time in the SSA method were concentrated at the corners of the search area (Fig. 10(e)). This concentration might contribute to the low value of R_{nearGS10}. These findings suggest that, except for the proposed and GS10 methods, the other methods struggle with parameter optimization in this uncertain context. The BA method requires a smaller N_{inv} than the proposed method. Both methods are based on the Bayesian optimization algorithm. Fig. 11 shows the representative results when comparing the number of investigations for each search parameter condition between the proposed and BA methods. In contrast to the BA method, which conduct only a single investigation per parameter, the proposed method frequently revisits certain parameters to refine their optimal values. These results demonstrate the effectiveness of the proposed method in attaining optimization with fewer searches, despite the low repeatability of the objective function values.

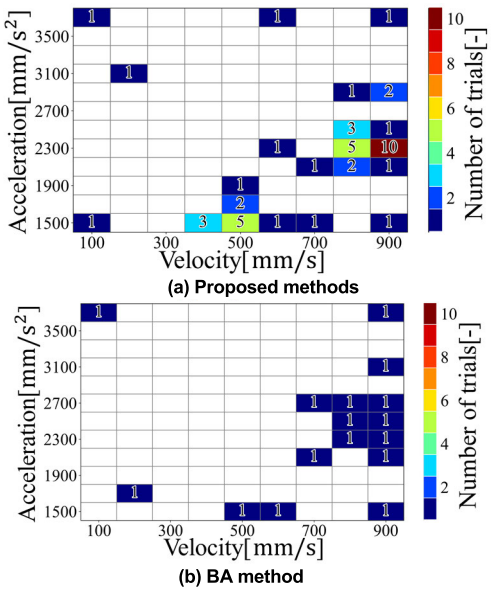

FIGURE 11. Representative results of the number of investigations for each search parameter condition.

Finally, the improvement in the productivity by the proposed method is discussed. From the results in Fig. 8, the number of cycles per day (N_{cy}) for the soft robotic hand system operating under the search parameter condition ($\boldsymbol{s}$) is calculated using

$$N_{cy}\left(\boldsymbol{s}\right) = \frac{60 \times 60 \times 24}{\mu_{GT}\left(\boldsymbol{s}\right)} \tag{32}$$

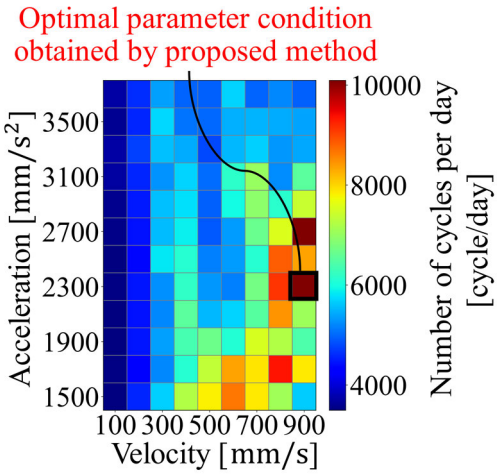

FIGURE 12. Numbers of cycles per day when the soft robotic hand system is operated under each search parameter condition.

As a reminder, $\mu_{GT}(\boldsymbol{s})$ denotes the means of the obtained cycle times for the search parameter condition $\boldsymbol{s}$. Fig. 12 shows the result. When the optimal search parameter $[\eta_{vel}, \eta_{acc}] = [900, 2300]$ was used for the operation, the N_{cy} value exceeded 10,000 cycles/day. To improve the productivity without optimizing the parameters, a typical approach would involve running the soft robotic hand system at the maximum speed and acceleration. In such a scenario, the parameter condition would be set to $[\eta_{vel}, \eta_{acc}] = [900, 3700]$, resulting in an N_{cy} value of approximately 5,000 cycles/day. This suggests that the proposed method achieves the reduction in N_{cy} of over 5,000 cycles/day compared to this scenario.

VII. CONCLUSION

This study introduced a novel parameter-tuning method for a soft robotic hand system to improve the cycle time of object transportational operations by considering the vibration of the robotic hand. This method identifies the optimal motion parameters for the manipulator that minimize the cycle time, accounting for the uncertainties due to the low repeatability of soft robotic hands. It employs sequential experimental exploration to identify the optimal parameters. To reduce the number of necessary investigations, this study developed a Bayesian-optimization-based search algorithm that systematically revisits previously explored parameters to enhance the reliability of the optimization criteria. In addition, a cost-effective and versatile measurement system was proposed to determine the vibration convergence time. This system utilizes a standard web camera with a resolution of 640 × 360 pixels and a frame rate of 30 fps, resulting in a cost-effective solution (26,180 JPY ≈ 183 USD). The camera, which served as an external sensor, enabled integration of the system into conventional robotic systems. The efficacy of the proposed motion optimization method was validated through comparisons with existing optimization techniques. The results confirmed that the proposed method effectively optimized the parameters of soft robotic hand systems. In this paper, the effectiveness of the proposed method for optimizing the motion in a soft robotic hand system was validated using a simple object-transportation task. Future work will aim to refine and expand this method for real-world applications by addressing more complex tasks, including grasping and placing. This may involve integrating sensory feedback and diverse actuators as well as incorporating more motion parameters for manipulator movements.

REFERENCES

[1] S. Puhlmann, J. Harris, and O. Brock, "RBO hand 3: A platform for soft dexterous manipulation," *IEEE Trans. Robot.*, vol. 38, no. 6, pp. 3434–3449, Dec. 2022.
[2] N. Feng, Q. Shi, H. Wang, J. Gong, C. Liu, and Z. Lu, "A soft robotic hand: Design, analysis, sEMG control, and experiment," *Int. J. Adv. Manuf. Technol.*, vol. 97, nos. 1–4, pp. 319–333, Jul. 2018.
[3] C. Lee, M. Kim, Y. J. Kim, N. Hong, S. Ryu, H. J. Kim, and S. Kim, "Soft robot review," *Int. J. Control, Autom. Syst.*, vol. 15, no. 1, pp. 3–15, Feb. 2017.
[4] D. Rus and M. T. Tolley, "Design, fabrication and control of soft robots," *Nature*, vol. 521, no. 7553, pp. 467–475, May 2015.
[5] Z. Wang and S. Hirai, "Soft gripper dynamics using a line-segment model with an optimization-based parameter identification method," *IEEE Robot. Autom. Lett.*, vol. 2, no. 2, pp. 624–631, Apr. 2017.
[6] X. Zhou, C. Majidi, and O. M. O'Reilly, "Soft hands: An analysis of some gripping mechanisms in soft robot design," *Int. J. Solids Struct.*, vols. 64–65, pp. 155–165, Jul. 2015.
[7] Q. Wang, W. Wang, L. Zheng, and C. Yun, "Force control-based vibration suppression in robotic grinding of large thin-wall shells," *Robot. Comput.-Integr. Manuf.*, vol. 67, Feb. 2021, Art. no. 102031.
[8] F. Chen, H. Zhao, D. Li, L. Chen, C. Tan, and H. Ding, "Contact force control and vibration suppression in robotic polishing with a smart end effector," *Robot. Comput.-Integr. Manuf.*, vol. 57, pp. 391–403, Jun. 2019.
[9] F. Ni, A. Henning, K. Tang, and L. Cai, "Soft damper for quick stabilization of soft robotic actuator," in *Proc. IEEE Int. Conf. Real-Time Comput. Robot. (RCAR)*, Jun. 2016, pp. 466–471.
[10] Y. Li, Y. Chen, T. Ren, and Y. Hu, "Passive and active particle damping in soft robotic actuators," in *Proc. IEEE Int. Conf. Robot. Autom. (ICRA)*, May 2018, pp. 1547–1552.
[11] H. Bilal, W. Yao, Y. Guo, Y. Wu, and J. Guo, "Experimental validation of fuzzy PID control of flexible joint system in presence of uncertainties," in *Proc. 36th Chin. Control Conf.*, Sep. 2017, pp. 4192–4197.
[12] Z. Mohamed and M. O. Tokhi, "Command shaping techniques for vibration control of a flexible robot manipulator," *Mechatronics*, vol. 14, no. 1, pp. 69–90, Feb. 2004.
[13] M. Busch, F. Schnoes, A. Elsharkawy, and M. F. Zaeh, "Methodology for model-based uncertainty quantification of the vibrational properties of machining robots," *Robot. Comput.-Integr. Manuf.*, vol. 73, Feb. 2022, Art. no. 102243.
[14] A. Abe, "Residual vibration suppression for robot manipulator attached to a flexible link by using soft computing techniques," in *Proc. IEEE Int. Conf. Robot. Biomimetics*, Dec. 2011, pp. 2324–2329.
[15] Y. Ueno and H. Tachiya, "Suppressing residual vibration caused in objects carried by robots using a heuristic algorithm," *Precis. Eng.*, vol. 80, pp. 1–9, Mar. 2023.
[16] Z. Pásztori, F. Ruggiero, V. Lippiello, and M. D. Castro, "Bayesian optimization approach to input shaper design for flexible beam vibration suppression," *IFAC-PapersOnLine*, vol. 53, no. 2, pp. 9150–9156, 2020.
[17] K. Yano, M. Hamaguchi, and K. Terashima, "Advanced control of liquid container transfer considering the suppression of liquid vibration," *IFAC Proc. Volumes*, vol. 30, no. 12, pp. 87–92, Jul. 1997.
[18] X. Wang, F. Li, Q. Du, Y. Zhang, T. Wang, G. Fu, and C. Lu, "Micro-amplitude vibration measurement using vision-based magnification and tracking," *Measurement*, vol. 208, Feb. 2023, Art. no. 112464.
[19] F. Wang, S. Hu, K. Shimasaki, and I. Ishii, "Real-time vibration visualization using GPU-based high-speed vision," *J. Robot. Mechatronics*, vol. 34, no. 5, pp. 1011–1023, Oct. 2022.

[20] D. Zhang, J. Guo, X. Lei, and C. Zhu, "A high-speed vision-based sensor for dynamic vibration analysis using fast motion extraction algorithms," *Sensors*, vol. 16, no. 4, p. 572, Apr. 2016.
[21] J. Li, D. Wang, X. Wu, K. Xu, and X. Liu, "Vibration prediction of the robotic arm based on elastic joint dynamics modeling," *Sensors*, vol. 22, no. 16, p. 6170, Aug. 2022.
[22] A. H. Khan and S. Li, "Sliding mode control with PID sliding surface for active vibration damping of pneumatically actuated soft robots," *IEEE Access*, vol. 8, pp. 88793–88800, 2020.
[23] H. Huang, G. Tang, H. Chen, J. Wang, L. Han, and D. Xie, "Vibration suppression trajectory planning of underwater flexible manipulators based on incremental kriging-assisted optimization algorithm," *J. Mar. Sci. Eng.*, vol. 11, no. 5, p. 938, Apr. 2023.
[24] P. Xin, J. Rong, Y. Yang, D. Xiang, and Y. Xiang, "Trajectory planning with residual vibration suppression for space manipulator based on particle swarm optimization algorithm," *Adv. Mech. Eng.*, vol. 9, no. 4, Apr. 2017, Art. no. 168781401769269.
[25] T. Nishimura, K. Mizushima, Y. Suzuki, T. Tsuji, and T. Watanabe, "Thin plate manipulation by an under-actuated robotic soft gripper utilizing the environment," in *Proc. IEEE/RSJ Int. Conf. Intell. Robots Syst. (IROS)*, Sep. 2017, pp. 1236–1243.
[26] S. Bai, J. Wang, F. Chen, and B. Englot, "Information-theoretic exploration with Bayesian optimization," in *Proc. IEEE/RSJ Int. Conf. Intell. Robots Syst. (IROS)*, Oct. 2016, pp. 1816–1822.
[27] P. I. Frazier, "A tutorial on Bayesian optimization," 2018, *arXiv:1807.02811*.
[28] J. Nogueira, R. Martinez-Cantin, A. Bernardino, and L. Jamone, "Unscented Bayesian optimization for safe robot grasping," in *Proc. IEEE/RSJ Int. Conf. Intell. Robots Syst. (IROS)*, Oct. 2016, pp. 1967–1972.
[29] H. Sasaki, T. Hirabayashi, K. Kawabata, Y. Onuki, and T. Matsubara, "Bayesian policy optimization for waste crane with garbage inhomogeneity," *IEEE Robot. Autom. Lett.*, vol. 5, no. 3, pp. 4533–4540, Jul. 2020.
[30] M. Feurer and F. Hutter, "Hyperparameter optimization," in *Automated Machine Learning* (Springer Series on Challenges in Machine Learning), F. Hutter, L. Kotthoff, and J. Vanschoren, Eds. Cham, Switzerland: Springer, 2019.
[31] Q. P. Nguyen, Z. Dai, B. K. H. Low, and P. Jaillet, "Optimizing conditional value-at-risk of black-box functions," in *Proc. Adv. Neural Inf. Process. Syst.*, vol. 6, 2021, pp. 4170–4180.
[32] Q. Phong Nguyen, Z. Dai, B. Kian Hsiang Low, and P. Jaillet, "Value-at-Risk optimization with Gaussian processes," 2021, *arXiv:2105.06126*.
[33] Soft Robotics Inc. *mGrip*. Accessed: Apr. 24, 2024. [Online]. Available: https://www.softroboticsinc.com/products/mgrip-modular-gripping-solution-for-machine-builders/?ref=steemhunt
[34] A. D. Marchese, R. K. Katzschmann, and D. Rus, "A recipe for soft fluidic elastomer robots," *Soft Robot.*, vol. 2, no. 1, pp. 7–25, Mar. 2015.
[35] C. Rossi and S. Savino, "Robot trajectory planning by assigning positions and tangential velocities," *Robot. Comput.-Integr. Manuf.*, vol. 29, no. 1, pp. 139–156, Feb. 2013.
[36] P. Auer, N. Cesa-Bianchi, and P. Fischer, "Finite-time analysis of the multiarmed bandit problem," *Adv. Neural Inf. Process. Syst.*, vol. 47, pp. 235–256, 2002.
[37] J. Kennedy and R. Eberhart, "Particle swarm optimization," in *Proc. Int. Conf. Neural Netw.*, vol. 4, 1995, pp. 1942–1948.
[38] J. Xue and B. Shen, "A novel swarm intelligence optimization approach: Sparrow search algorithm," *Syst. Sci. Control Eng.*, vol. 8, no. 1, pp. 22–34, Jan. 2020.
[39] M. A. Awadallah, M. A. Al-Betar, I. A. Doush, S. N. Makhadmeh, and G. Al-Naymat, "Recent versions and applications of sparrow search algorithm," *Arch. Comput. Methods Eng.*, vol. 30, no. 5, pp. 2831–2858, 2023.

TOSHIHIRO NISHIMURA (Member, IEEE) received the B.S., M.S., and Ph.D. degrees in mechanical engineering from Kanazawa University, Kanazawa, Japan, in 2016, 2018, and 2019, respectively. He was a Researcher of industrial robots with FANUC Corporation, from 2018 to 2021. He is currently an Assistant Professor with the Faculty of Frontier Engineering, Institute of Science and Engineering, Kanazawa University. His research interests include robotic hands, mechanism design, soft robotics, and 3-D printer.

TATSUKI ISOGAI received the B.S. degree from Kanazawa University, in 2022. He is currently pursuing the degree with the Department of Frontier Engineering, Graduate School of Natural Science and Technology, Kanazawa University, Kanazawa, Japan. His research interests include soft robotic and motion optimization.

YOSUKE SUZUKI (Member, IEEE) received the B.Eng., M.Eng., and Ph.D. degrees in engineering from Tokyo Institute of Technology, Tokyo, Japan, in 2005, 2007, and 2010, respectively. He is currently an Assistant Professor with the Faculty of Mechanical Engineering, Institute of Science and Engineering, Kanazawa University, Kanazawa, Japan. His research interests include tactile and proximity sensors, robotic grasping, and distributed autonomous systems.

TOKUO TSUJI (Member, IEEE) received the B.S., M.S., and Ph.D. degrees from Kyushu University, in 2000, 2002, and 2005, respectively. He was a Research Fellow with the Graduate School of Engineering, Hiroshima University, from 2005 to 2008. He was a Research Fellow with the Intelligent Systems Research Institute, National Institute of Advanced Industrial Science and Technology (AIST), from 2008 to 2011. From 2011 to 2016, he was a Research Associate with Kyushu University. Since 2016, he has been working as an Associate Professor with the Institute of Science and Engineering, Kanazawa University. His research interests include multifingered hand, machine vision, and software platform of robotic systems.

TETSUYOU WATANABE (Member, IEEE) received the B.S., M.S., and Dr.Eng. degrees in mechanical engineering from Kyoto University, Kyoto, Japan, in 1997, 1999, and 2003, respectively. From 2003 to 2007, he was a Research Associate with the Department of mechanical Engineering, Yamaguchi University, Japan. From 2007 to 2011, he was an Assistant Professor with the Division of Human and Mechanical Science and Engineering, Kanazawa University. From 2008 to 2009, he was a Visiting Researcher with Munich University of Technology. From 2011 to 2018, he was an Associate Professor with the Faculty of Mechanical Engineering, Institute of Science and Engineering, Kanazawa University. Since 2018, he has been a Professor with Kanazawa University. His current research interests include robotic hand, grasping, object manipulation, medical sensors, surgical robots, and user interface.